

Development of tungsten fibre-reinforced tungsten composites towards their use in DEMO – Potassium doped tungsten wire

J Riesch^{1,*}, Y Han¹, J Almanstötter³, J W Coenen², T Höschen¹, B Jasper², P Zhao¹,
Ch Linsmeier² and R Neu^{1,4}

¹ Max-Planck-Institut für Plasmaphysik, 85748 Garching, Germany

² Forschungszentrum Jülich GmbH, Institut für Energie und Klimaforschung – Plasmaphysik, 52425 Jülich,
Germany

³ OSRAM GmbH, Corporate Technology CT TSS MTS MET, 86830 Schwabmünchen, Germany

⁴ Fakultät für Maschinenbau, Technische Universität München, D-85748 Garching, Germany

*Corresponding author: johann.riesch@ipp.mpg.de

Abstract. For the next step fusion reactor the use of tungsten is inevitable to suppress erosion and allow operation at elevated temperature and high heat loads. Tungsten fibre-reinforced composites overcome the intrinsic brittleness of tungsten and its susceptibility to operation embrittlement and thus allow its use as a structural as well as an armour material. That this concept works in principle has been shown in recent years. In this contribution we present a development approach towards their use in a future fusion reactor. A multilayer approach is needed addressing all composite constituents and manufacturing steps. A huge potential lies in the optimization of the tungsten wire used as fibre. We discuss this aspect and present studies on potassium doped tungsten wire in detail. This wire, utilized in the illumination industry, could be a replacement of the so far used pure tungsten wire due to its superior high temperature properties. In tensile tests the wire showed high strength and ductility up to an annealing temperature of 2200 K. The results show that the use of doped tungsten wire could increase the allowed fabrication temperature and the overall working temperature of the composite itself.

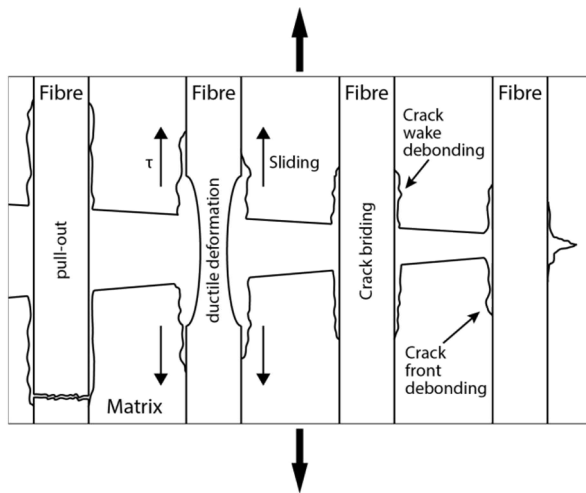
1. Introduction

29 Materials with advanced capabilities are essential for the successful design of the next step
30 fusion reactor, i.a. DEMO, and are crucial for a fusion power plant. The use of tungsten is
31 inevitable to suppress erosion and to allow operation at elevated temperature and high heat
32 loads [1]. However tungsten suffers from an intrinsic brittleness below a certain temperature,
33 the so called ductile-to-brittle transition temperature [2,3]. Depending on mechanical,
34 chemical and (micro-)structural conditions this temperature is between 500 and 900 K. In
35 addition W is susceptible to be further embrittled by overheating or neutron irradiation [4].

36 Tungsten fibre-reinforced tungsten composites (W_f/W) utilize extrinsic toughening
37 mechanisms like crack bridging by intact fibres or frictional pull-out of broken fibres. Similar
38 to ceramic fibre-reinforced ceramics [5] the overall toughness is increased and the brittleness
39 problem of W is mitigated. Hence an application as a plasma facing material under thermal
40 transients and neutron bombardment now seems feasible.

41 That extrinsic toughening works in W_f/W has been shown at the Max-Planck-Institute for
42 Plasma Physics, Garching (IPP) in the past years [6,7]. As a key factor for the feasibility of
43 this toughening mechanism the interface between fibre and matrix was investigated in a first
44 step [8,9]. The feasibility of the toughening effect itself was shown on model systems
45 consisting of a single fibre embedded in the matrix material. With this method the major
46 contribution of the plastic fibre deformation to the toughening was shown [10]. In addition it
47 was proven that the toughening mechanisms are still active after a full change of the
48 microstructure by recrystallization [11]. Figure 1 shows a summary of the active toughening
49 effects in W_f/W . In a further development step a fabrication method based on the chemical
50 deposition of W was developed and first bulk samples were produced [12]. Mechanical tests
51 on these samples revealed an intense toughening. Based on these results the material was
52 chosen as risk mitigation PFC/HHF (plasma facing component/high heat flux) material in the
53 EU Fusion roadmap [13]. In summary the idea of extrinsic toughening in W works in
54 principle and the application as highly loaded divertor element is identified. Thus level 2 of

55 the so called technology readiness level (TRL) is reached (proof-of-principle + application
56 formulated) (explanation of TRL concept in [14]).



57

58 *Figure 1: Toughening mechanism in tungsten fibre-reinforced composites.*

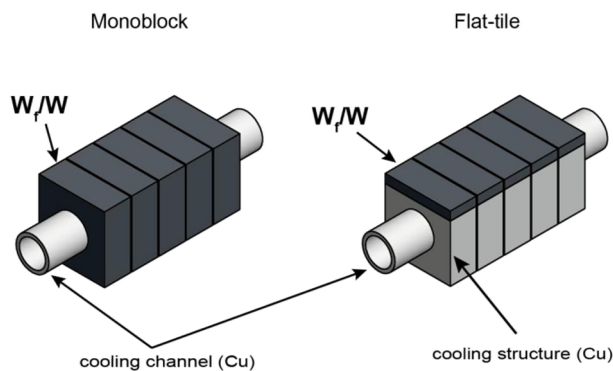
59

60 Candidate materials for DEMO however need to reach TRL 6-8 before being considered for
61 design [15]. The first step in this development is to prove that the concept of a W_f/W divertor
62 element works (TRL3, proof-of-concept) and to validate it under relevant testing conditions
63 (TRL4, validation). TRL 5 is typically associated with the validation in a relevant
64 environment. In the case of W_f/W this is associated with the plasma interaction, e.g. regarding
65 hydrogen retention or erosion, and the behavior under neutron irradiation. TRL 6 will be
66 reached by a prototype demonstration in a relevant environment. This can be in wall tiles of
67 existing fusion reactors, e.g. on a manipulator or as a long term wall tile.

68 As a first step it has been chosen to fabricate W_f/W components and test them under cyclic
69 high heat flux conditions. These components will be designed close to the ITER reference-
70 design. In figure 2 two possible versions for such a mock-up are shown. The loading will be
71 performed in the ion beam facility GLADIS in Garching, Germany [16,17] and/or the electron
72 beam facility JUDITH 1 [18]. Cyclic extreme loading allows the evaluation of the maximum
73 strength, the fatigue strength and the damage tolerance/toughness and thus provides the
74 conceptual proof in one step. The concentration on one main test provides clear constraints

75 for geometry and test methodology. This leads to a distinct structure and allows a target-
76 oriented approach. For the successful realization and evaluation of such experiments the
77 complete characterization of the material is essential. In summary this allows not only to
78 show that the concept works but also qualifies W_f/W for future applications, e.g. in a DEMO
79 divertor (TRL 4).

80



81

82 *Figure 2: Monoblock and Flat tile mock-up for high heat flux tests*

83

84 For the component production and the following testing all constituents of the composite, i.a.
85 fibre, interface and matrix, and all manufacturing steps, i.a. interface coating, fibre positioning
86 and matrix production, will be addressed. Utilizing the so far used techniques, a pure tungsten
87 fibre, an oxidic interface and a chemically deposited matrix as a starting point, new
88 techniques will be investigated and/or established techniques will be optimized. As all these
89 aspects are strongly linked, e.g. the manufacturing temperature of the W matrix with the high
90 temperature stability of the W fibre or the interface, this is a multilayer approach.

91 As an example we discuss in this paper the role of the tungsten wire used as fibre and
92 especially the influence of annealing on its mechanical properties. A screening test on
93 potassium doped tungsten wire is presented in detail. As this is strongly related to the allowed
94 matrix manufacturing temperatures, a short review is given on matrix production techniques
95 at first.

96

97 **2. Fabrication of the tungsten matrix in W_f/W composites**

98 The very high melting point and high temperature strength both for fibre and matrix do not
99 allow for classical composite production routes (examples in [5]). It is furthermore important
100 that the properties of fibre and interface are not degraded during the process. Chemical
101 deposition techniques allow low processing temperatures (< 900 K) and a force-less
102 fabrication, and thus the preservation of the interface and fibre integrity as well as fibre
103 topology. In this process tungsten hexafluoride is reduced by hydrogen in a heterogeneous
104 surface reaction and thus solid tungsten is formed.

105 So far surface deposition processes (chemical vapour deposition – CVD) have been used for
106 the production of model systems containing a single fibre [8] and infiltration techniques
107 (chemical vapour infiltration – CVI) have been investigated to produce larger samples. The
108 infiltration process can be influenced by varying the fibre arrangement, the gas flow and the
109 temperature. In a dual step infiltration process Riesch et al. were able to produce first bulk
110 W_f/W for mechanical testing [12]. A key issue is the optimization of this tungsten matrix
111 production process allowing the production of larger, reproducible samples. A chemical
112 deposition device (WILMA) which has been specifically designed for the chemical deposition
113 of tungsten for the matrix production in W_f/W was installed at the Forschungszentrum Jülich
114 (FZJ).

115 Although CVD processes have the advantage of low production temperature and the absence
116 of mechanical impact, powder metallurgical (PM) routes would allow several interesting
117 benefits. The most important benefit is that the production and processing techniques are
118 highly developed as PM is the standard process for tungsten bulk production. This would give
119 potential for an easier optimisation and adoption of the matrix properties. For example it
120 would be easier to implement alloying, e.g. self passivating tungsten. Nevertheless the

121 required high temperature and pressure might be a severe drawback regarding degradation of
122 fibre or interface properties.

123 PM investigations on single fibre composites have been started in order to understand the
124 interaction between fibre, interface and matrix. Hot isostatic pressing (HIP) was applied to
125 produce a dense W matrix with and without embedded fibres. First samples at various HIPing
126 temperature up to 2200 K have been produced and mechanical testing including fibre push out
127 has been performed. These tests show that the interface properties are critical for the path
128 forward within the HIPing approach. A detailed description of these tests and their results is
129 given by Jasper et al. [19].

130 In these tests pure tungsten wire was used as fibres. These fibres were fully recrystallized
131 during the HIP process. As recrystallized fibres possess very poor mechanical properties
132 compared to as-fabricated ones [20] this is a severe drawback for PM production route. As a
133 loophole potassium doped fibres are known for their high temperature stability and could be a
134 solution. In the following we present experiments on the mechanical properties after high
135 temperature annealing to investigate this option.

136

137 **3. Mechanical properties of W-wire used as fibre in W_f/W composites**

138 A key benefit of W_f/W under cyclic high heat loads are the exceptional properties of the
139 tungsten wires used as fibres: Pure as well as potassium doped tungsten wires show
140 exceptional ductility and strength at room temperature in contrast to conventional bulk
141 tungsten being brittle at room temperature. These are ideal properties facilitating the
142 toughening in W_f/W as the high strength is important for the bridging effect and ductile
143 deformation allows the dissipation of substantial amount of energy (compare mechanism in
144 figure 1).

145 Pure tungsten wires have been investigated by Zhao et al. [20] by means of tensile tests.
146 Wires in the as-fabricated state and after annealing for 3 h at 1273 K and 30 minutes at 1900

147 K were tested. The as-fabricated and the low heat treated fibres showed ductile behaviour and
148 a strength of more than 2900 MPa and 1900 MPa respectively. In contrast to that the high
149 temperature heat treated fibres failed in a brittle manner with a mean strength of
150 approximately 900 MPa, and a high scatter. In the following we present similar experiments
151 on potassium doped tungsten wire.

152 *3.1 Sample preparation*

153 Drawn tungsten wire doped with 60-75 ppm potassium was used for tensile tests. The wire
154 was produced and provided by the OSRAM GmbH, Schwabmünchen. The measured diameter
155 of the wire was $148.7 \pm 0.2 \mu\text{m}$. The wire was cut into pieces and straightened by tensile
156 loading until fracture (displacement rate of $100 \mu\text{m/s}$). The straightened wires were cut into
157 80 mm long pieces to get rid of the damaged zone. The 80 mm wire pieces are called fibres in
158 the following.

159 Fibres in the as-fabricated state and after annealing were tested. 5 different annealing
160 temperatures are investigated (see table 1). The annealing was done in a tube furnace under
161 hydrogen atmosphere. The holding time was 30 min in each case.

162 Temperature 1-3 are below the reported temperature of extensive grain growth in potassium
163 doped wire (2100-2300 K [21]), temperature 4 is around this region and temperature 5 is well
164 above it. In addition temperature 1 and 3 are similar to the annealing temperatures in pure
165 tungsten wire studies [20] and therefore allow a direct comparison.

166 In figure 3 optical micrographs of longitudinal sections are shown for the different sample
167 types. The extensive grain growth leading to very big grains is clearly visible for the sample
168 annealed at 2573 K.

169

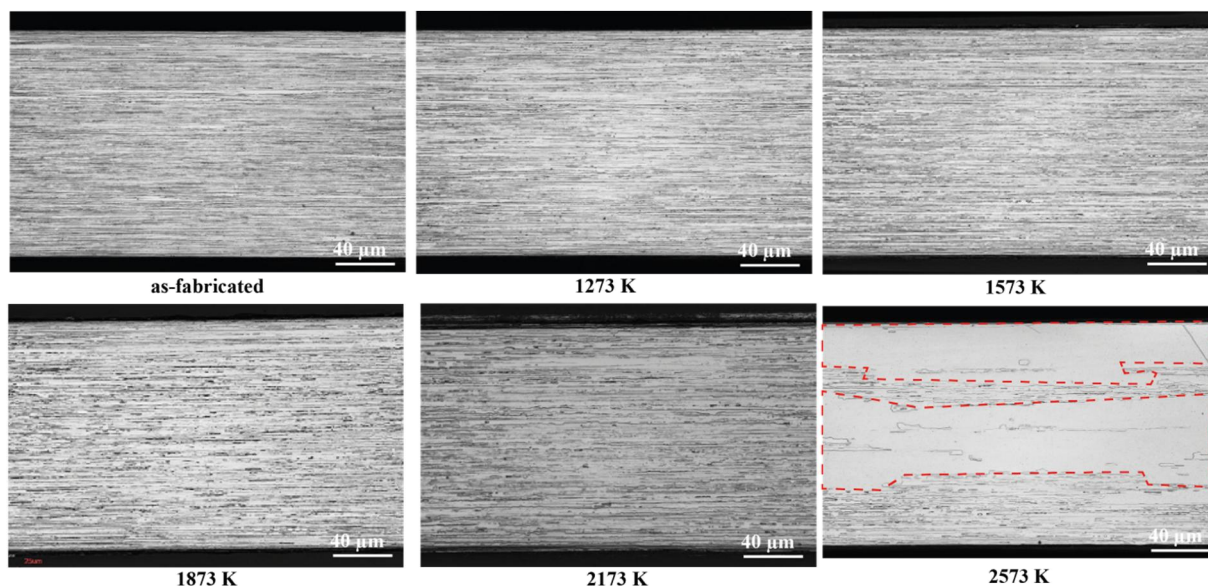
170 *Table 1: Annealing temperature*

<i>T 0</i>	<i>T 1</i>	<i>T 2</i>	<i>T 3</i>	<i>T 4</i>	<i>T 5</i>
------------	------------	------------	------------	------------	------------

Annealing

<i>temperature</i>	-	1273	1573	1873	2173	2573
<i>[K]</i>						

171



172

173 *Figure 3 Longitudinal sections (optical) of potassium doped tungsten wire at different*
 174 *annealing stages. The dashed lines in the 2573 K case indicate large grains after secondary*
 175 *grain growth.*

176

177 *3.2 Experimental*

178 The tensile tests were performed with a universal testing machine (TIRA Test 2820) at room
 179 temperature. The load is measured by a 200 N range load cell. The displacement was
 180 measured contactless by a laser speckle extensometer (LSE-4000 DE) using the interference
 181 pattern of two laser spots. This measurement requires a perfectly aligned sample. To align the
 182 fibre within the tension axis a preload (between 10-15 N \cong 550-850 MPa) is applied and the
 183 lower sample holder is moved until a load minimum is reached. Still the displacement record
 184 was not always reliable.

185 The measuring length is defined by the distance between the two laser spots and was
186 approximately 18 mm for all tests. Only if the fibre fractures within this zone the test is
187 assigned as valid. To ensure that the fibre fractures within the measuring length both ends of
188 the fibre are attached to paper by gluing (UHU Plus endfest 300). Thus the cross-section in
189 these parts is enlarged and the probability of fracture is decreased. The uncovered part was
190 approximately 20 mm for all tests. The tests were conducted in a displacement controlled
191 mode with a displacement rate of 5 $\mu\text{m/s}$.

192

193 **4. Results**

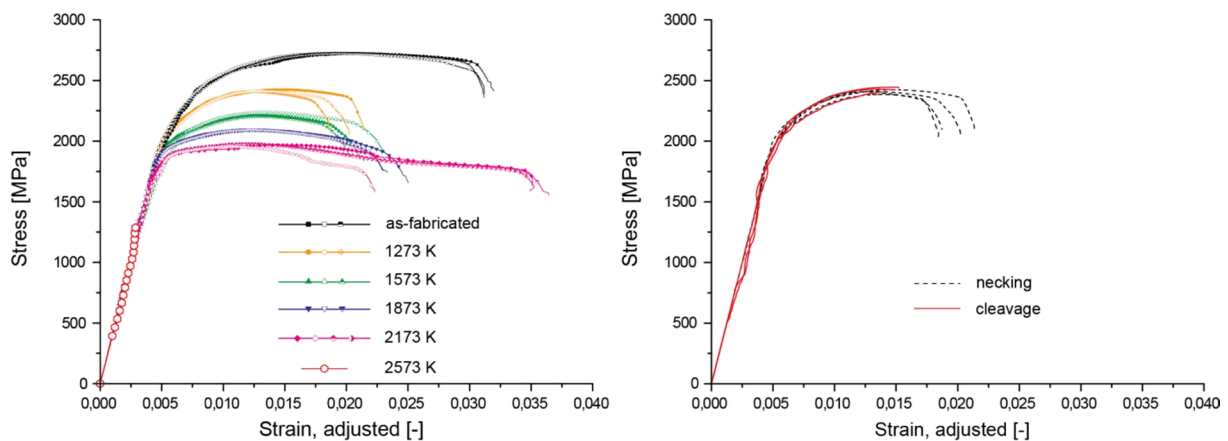
194 Figure 4 (left) shows typical stress-strain curves of the tested wires. The region of elastic
195 response was extrapolated to the origin (dotted line). Due to unreliable strain measurements
196 the estimated Young's moduli show significant deviation between 280 and 440 GPa. To be
197 able to compare the different annealing stages the strain axis was corrected to meet 400 GPa
198 in the elastic region. However as the variations are quite significant we do not give any
199 quantitative values besides the ultimate strength which is independent of the displacement
200 measurement. Nevertheless trends are obvious for other mechanical properties like yield
201 strength and fracture strain.

202 In all cases an elastic deformation is observed for low strain. Except for the 2573 K case this
203 is followed by an extended phase of plastic deformation. If plastic deformation occurs the
204 stress decreases moderately after reaching the ultimate strength. This goes on until a faster
205 drop occurs near final fracture. Samples annealed at 1273K do not show this drop in 8 out of
206 24 cases and fail near to the maximum load. Typical curves for both cases are shown in
207 Figure 4 (right). However yield strength and ultimate strength of these samples are
208 comparable. The mean value for the ultimate strength of the different sample types is given in
209 table 2. The errors are calculated by the standard deviation of the mean. For each temperature

210 6 valid measurements are considered. 16 samples have been taken into account for annealing
 211 temperature of 2573 K to give a better statistic in the brittle case.

212 In the as-fabricated case work hardening of approximately 2 % is observed. The work
 213 hardening becomes less with increased annealing temperature. For the samples annealed at
 214 2173 K almost no work hardening is observed. The fracture strain drops with the first
 215 annealing step and stays almost constant for the next higher temperatures. For the annealing
 216 temperature of 2173 K it increases significantly and is even larger as in the as-fabricated case.
 217 However one out of 6 tested samples shows a lower fracture strain at this annealing stage. The
 218 yield strength as well as the ultimate strength decrease with rising annealing temperature.

219



220

221 *Figure 4: Typical stress-strain curves of tensile tests of potassium doped tungsten wire at*
 222 *different annealing stages (left). Three samples are shown for the as-fabricated case and an*
 223 *annealing temperature of 1273 K, 1573 K and 1873 K. A fourth sample having a much lower*
 224 *fracture strain is shown for annealing temperatures 2173 K. For the sake of clarity only one*
 225 *curve is shown for temperature 2573 K. For an annealing temperature of 1273 K fracture*
 226 *with necking as well as cleavage dominated occurred (right).*

227

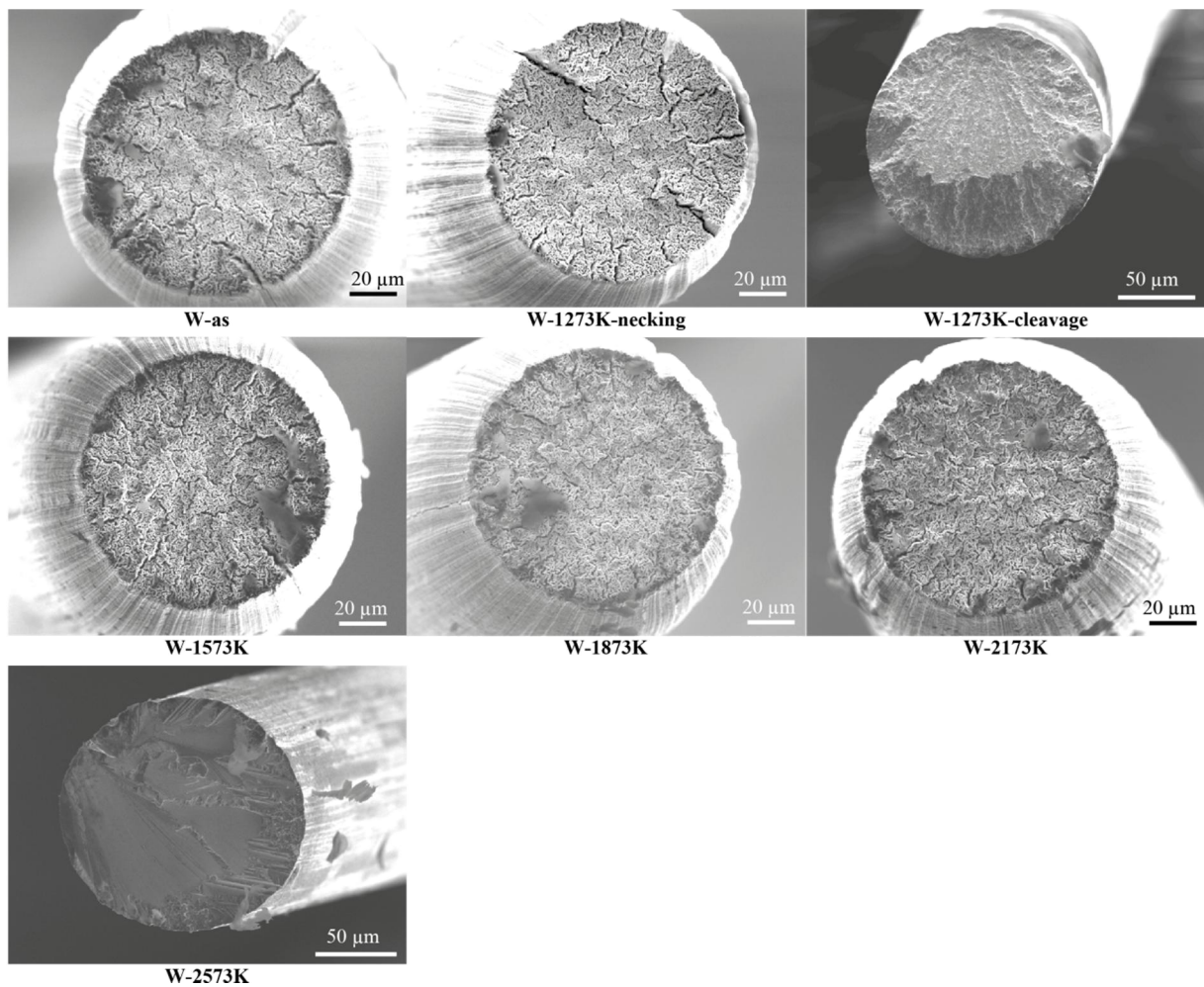
228 *Table 2: Ultimate strength of potassium doped tungsten wire with different annealing stages*
 229 *determined in tensile tests.*

	<i>W-as</i>	<i>W-1273K</i>	<i>W-1573K</i>	<i>W-1873K</i>	<i>W-2173K</i>	<i>W-2573K</i>
<i>Ultimate Strength [MPa]</i>	2721±1	2409±6	2220±5	2089±4	1968±4	1274±26

230

231 Typical fracture surfaces for each sample type are shown in figure 6. Almost all fibres show
 232 necking (reduction in cross-section) and a fibrous, knife edge necking dominated fracture
 233 mode. Samples annealed at 1273 K without necking (missing step stress drop at the end of
 234 tension test) and annealed at 2573 K show a cleavage dominated fracture.

235



236

237 *Figure 5: Typical fracture surfaces after tensile tests of potassium doped tungsten wire with*
 238 *different annealing stages.*

239

240 **5. Discussion**

241 Most of the samples with an annealing temperature up to 2173 K show ductile behaviour with
242 significant plastic deformation, a high fracture strain and pronounced necking. The fracture
243 surfaces for these samples are typical for the ductile fracture of tungsten wire [22]. At first
244 longitudinal grain boundaries debond leading to freestanding individual grains. Afterwards
245 these grains neck down in a knife-edge fracture mode leading to a typical fibrous surface. For
246 some samples annealed at 1273 K ductile behaviour without a dedicated necking regime is
247 observed. These samples show a cleavage dominated fracture mode. All samples annealed at
248 2573 K show pure elastic i.e. brittle behaviour with a cleavage dominated fracture mode.

249 To understand this behaviour the annealing behaviour and accordingly the recrystallization
250 behaviour are important. Recrystallisation is difficult to tackle in doped tungsten wire as the
251 processes are different compared to pure bulk tungsten [23]. Two distinct stages are
252 identified: at first a relatively uniform coarsening sometimes referred to as primary
253 recrystallization (starting at 1100 K) followed by a rapid growth of large elongated grains
254 referred as secondary recrystallization or extensive grain growth (starting at 2200 K) [24].
255 The first stage is assigned to polygonisation in which dislocations are organized into low
256 angle boundaries [22] but also at this stage high angle boundary migration is active [25]. At
257 the same time potassium bubble rows are formed at the grain boundaries inhibiting grain
258 boundary migration in the radial direction. Thus the elongated grain structure is retained
259 during grain coarsening until some grains reach the critical size (Hillerts criteria [26]) and
260 show rapid grain growth. Also dragging of bubbles at this temperature can contribute to that
261 effect [25].

262 As long as a relatively fine and elongated grain structure is preserved the amount of grain
263 boundaries perpendicular to the tension load is small. Even if such boundaries debond they
264 are bridged by adjacent long grains leading to a ductile behaviour. This seems to be the case
265 until secondary grain growth occurs. The embrittlement is correlated with the occurrence of
266 very large grains which facilitate cleavage.

267 In samples which were annealed at 1273 K, the reasons for the occurrence of cleavage and
268 therefore the missing of necking are not obvious. For the occurrence of the knife edge fracture
269 grain boundary debonding is necessary. The weakening of these boundaries by the formation
270 of the potassium bubbles or by the interaction of longitudinal grain boundaries with these
271 bubbles at increasing annealing temperature might be beneficial. In the as-fabricated stage the
272 dislocations, which are present in a high amount, are able to move to the grain boundaries
273 during loading and might have similar effects. The occurrence of cleavage at 1273 K
274 annealing temperature is probably caused by a complicated interaction between annihilation
275 of dislocations and formation of bubble rows and needs further investigation.

276 The as-fabricated wire shows a more pronounced strain hardening behaviour which can be
277 attributed to the high density of dislocations due to the drawing process. With ongoing heat
278 treatment the dislocation density decreases due to annihilation and grain coarsening.
279 Therefore the blocking of dislocations is less pronounced and thus the work hardening rate is
280 lower. For the same reason the yield strength decreases with rising annealing temperature.
281 The strength stays around 2000 MPa until the very high annealing temperature where
282 extensive grain growth and brittle behaviour occurs. All samples annealed at 1273 K show the
283 same strength independent of the occurrence of necking. That means that there is no
284 significant difference in the onset of ductile deformation. Leber et. al [22] also reported
285 ductile deformation prior to cleavage fracture.

286
287 The strength in the as-fabricated state is slightly smaller than reported previously for pure
288 tungsten wire in similar tests [20]. The strength is influenced very much by the deformation
289 rate and the annealing stages during fabrication [27] and was also reported to be higher in
290 doped W wire in some cases [28]. Different fabrication histories are therefore most probably
291 the cause for the differences in strength. The effect of decreasing work hardening capability
292 with rising temperature is similar in both cases. The gain in fracture strain observed for doped

293 wires is not reported for pure W wire. This might be attributed to having fewer annealing
294 stages but could also be caused by the faster loss of the elongated grain structure. The fracture
295 modes are similar, knife necking of individual grains in the ductile case and cleavage
296 dominated fracture in the brittle case. In pure W wire the embrittlement was correlated with
297 the loss of elongated grain structure and not necessarily with the occurrence of
298 recrystallization. Samples annealed at 1273K showed clear evidence of recrystallization but
299 also clear ductile behaviour. This was attributed to the preserved elongated grain structure. In
300 samples annealed at 1900 K this elongated structure was lost and the samples showed brittle
301 behaviour. The elongated grain structure was therefore identified to be the key factor deciding
302 whether there is ductile or brittle behaviour. In contrast to that the size of the grains plays an
303 additional role in potassium doped wire. Very large grains provoke brittle fracture even
304 though they are elongated. This size effect was probably not observed in pure W wire as here
305 the grains lose their elongated shape much earlier due to the absences of the grain boundary
306 pinning by potassium.

307 In summary similar effects seem to be valid in both pure and potassium doped tungsten wire.
308 Annealing and even recrystallization leads at first to a decrease in work hardening capability
309 most probably due to the decrease in dislocation density but not necessarily to embrittlement.
310 Both types show ductile behaviour as long as an elongated fine grain structure is preserved.
311 The main difference is that due to the potassium doping grain boundaries are pinned and this
312 structure is preserved to much higher temperatures compared up to pure tungsten wire.

313

314 **6. Conclusion and outlook**

315 Tungsten fibre-reinforced composites feature unique properties which could allow their use in
316 highly loaded areas of a future fusion reactor. However to reach this goal further development
317 steps are necessary. The first step will be reached by producing mock-ups and testing them
318 under cyclic high heat load. For this a multilayer approach is necessary addressing all

319 composite constituents and relevant manufacturing techniques. As an example the role of the
320 tungsten wire used as fibre is discussed as for instance the properties of the wire are not only
321 important for the composite properties but are also constraining the fabrication process.

322 Potassium doped tungsten wire was investigated by means of tensile tests in the as-fabricated
323 and annealed states in order to investigate its use as fibre reinforcement in W_f/W . The main
324 findings are:

- 325 • Potassium doped W wire annealed up to 2173 K shows ductile behaviour.
- 326 • Tensile strength stays about 2000 MPa up to annealing temperatures of 2173 K.
- 327 • Secondary grain growth at 2573 K leads to embrittlement

328 Similar to pure tungsten wire embrittlement is correlated with the loss of the fine elongated
329 grain structure. To achieve a better understanding of the correlation between microstructure,
330 i.a. dislocation density, grain size and aspect ratio, and mechanical behaviour a detailed
331 EBSD study could be performed on the samples.

332 As potassium doped wire does not lose its good mechanical properties and in particular its
333 ductile behaviour up to very high temperature the fabrication temperature of W_f/W
334 composites could be significantly increased. In addition the results are a strong indication that
335 the application temperature of W_f/W might be increased if using doped wire. This has to be
336 proven by investigating the mechanical properties of annealed W_f/W samples and by tensile
337 tests of potassium doped W wire at an elevated temperature.

338

339 **Acknowledgements**

340 The authors want to acknowledge support by Osram GmbH, Schwabmünchen, Germany for
341 providing the tungsten wire and M. Fuhr for his assistance in the metallographic preparations.

342 This work has been carried out within the framework of the EUROfusion Consortium and has
343 received funding from the Euratom research and training programme 2014-2018 under grant

344 agreement No 633053. The views and opinions expressed herein do not necessarily reflect
345 those of the European Commission.

346

347 **References**

- 348 [1] Coenen et al. Materials for DEMO and Reactor Applications - Boundary Conditions and New Concepts.
349 *submitted to Physica Scripta (in this volume)*, PHYSSCR-103131, 2015
- 350 [2] N. Baluc. Final report on the EFDA task tw1-ttma-002 deliverable 5. *Technical report, Centre de*
351 *Recherches en Physique de Plasmas*, 2002.
- 352 [3] R. Lässer, N. Baluc, J.-L. Boutard, E. Diegele, S. Dudarev, M. Gasparotto, A. Möslang, R. Pippan, B.
353 Riccardi, and B. van der Schaaf. Structural materials for DEMO: The EU development, strategy, testing
354 and modelling. *Fusion Engineering and Design*, **82**:511–520, 2007.
- 355 [4] J.-H. You and I. Komarova. Probabilistic failure analysis of a water-cooled tungsten divertor: Impact of
356 embrittlement. *Journal of Nuclear Materials*, **375**:283–289, 2008.
- 357 [5] K.K. Chawla. Ceramic matrix composites. *Chapman & Hall*, 1993.
- 358 [6] J. Du. A Feasibility Study of Tungsten-Fiber-Reinforced Tungsten Composites with engineered
359 interfaces. *Ph.D thesis, Technische Universität München*, 2011,
360 <http://mediatum.ub.tum.de/node?id=998317>
- 361 [7] J. Riesch. Entwicklung und Charakterisierung eines wolframfaserverstärkten Wolfram-
362 Verbundwerkstoffs. *Ph.D. thesis, Technische Universität München*, 2012,
363 <http://mediatum.ub.tum.de/node?id=1106428>
- 364 [8] J. Du, T. Höschen, M. Rasinski, S. Wurster, W. Grosinger, and J.-H. You. Feasibility study of a tungsten
365 wire reinforced tungsten matrix composite with ZrO_x interfacial coatings. *Composites Science and*
366 *Technology*, **70**:1483-1489, 2010.
- 367 [9] J. Du, T. Höschen, M. Rasinski, and J.-H. You. Interfacial fracture behavior of tungsten wire/tungsten
368 matrix composites with copper-coated interfaces. *Materials Science and Engineering: A*, **527**:1623–
369 1629, 2010.
- 370 [10] J. Riesch, J.-Y. Buffiere, T. Höschen, M. di Michiel, M. Scheel, Ch. Linsmeier, and J.-H. You. In-situ
371 synchrotron tomography estimation of toughening effect by semi-ductile fibre reinforcement in a
372 tungsten fibre-reinforced tungsten composite system. *Acta Materialia*, **61**:7060–7071, 2013.

- 373 [11] J. Riesch, J.-Y. Buffière, T. Höschen, M. Scheel, and J.-H. You. Crack bridging in as-produced and
374 embrittled tungsten single fibre reinforced tungsten composites shown by a novel in-situ high energy
375 synchrotron tomography bending test. *submitted to Acta Materialia*.
- 376 [12] J. Riesch, T. Höschen, Ch. Linsmeier, S. Wurster, and J-H You. Enhanced toughness and stable crack
377 propagation in a novel tungsten fibre-reinforced tungsten composite produced by chemical vapour
378 infiltration. *Physica Scripta*, **T159**:014031 (7pp), 2014.
- 379 [13] Materials Assessment Group. Assessment of the EU R&D Programme on DEMO Structural and High-
380 Heat Flux Materials. Final report. 2012.
- 381 [14] Mankins, J.C.. Technology readiness assessments: A retrospective. *Acta Astronautica*, **65**:1216-
382 1223,2009.
- 383 [15] D. Stork. Developing Structural, High-heat flux and Plasma Facing Materials for a near-term DEMO
384 Fusion Power Plant: the EU Assessment. *16th International Conference on Fusion Reactor Materials*,
385 Beijing, 2013.
- 386 [16] H. Greuner et al. Design, performance and construction of a 2MW ion beam test facility for plasma
387 facing components. *Fusion Engineering and Design*, **75–79**:345–350, 2005.
- 388 [17] H. Greuner, B. Böswirth, J. Boscary und P. McNeely. High heat flux facility GLADIS: Operational
389 characteristics and results of W7-X pre-series target tests. *Journal of Nuclear Materials*, **367–370**:1444–
390 1448, 2007.
- 391 [18] R. Duwe, W. Kühnlein, and H. Münstermann. The new Electron Beam Facility for Materials Testing in
392 Hot Cells. *Fusion Technology*, 356-358, 1995.
- 393 [19] B. Jasper, J.W. Coenen, J. Riesch, T. Höschen, M. Bram, and Ch. Linsmeier. Powder Metallurgical
394 Tungsten Fiber-Reinforced Tungsten. *Materials Science Forum*, Vols **825-826**:125-133, 2015.
- 395 [20] P. Zhao, J. Riesch, T. Höschen, J. Almanstötter M. Balden, J.W. Coenen, and R. Neu. Microstructure,
396 mechanical behavior and fracture of pure tungsten wires after different heat treatments. *submitted to*
397 *International Journal of plasticity*.
- 398 [21] C.L. Briant, O. Horacek, and K. Horacek. The Effect of Wire History on the Coarsened Substructure
399 and Secondary Recrystallization of Doped Tungsten. *Metallurgical Transactions A*. 24A:849-851 ,
400 1993.
- 401 [22] S. Leber, J. Tavernelli, and D.D. White. Fracture modes in tungsten wire. *Journal of the Less-Common*
402 *Metals*, **48**:119-133, 1976.

- 403 [23] L. Uray, A. Sulyok, and P. Tekula-Buxbaum. Factors Influencing the Recrystallization of Non-Sag
404 Tungsten Wires Indicated by the Out-Diffusion of Cobalt. *High Temperature Materials and Processes*,
405 **24-5**:289-299, 2005.
- 406 [24] D.B. Snow. The recrystallization of non-sag tungsten wire. In The metallurgy of doped/non-sag
407 tungsten. *Elsevier Applied Science*, 1989
- 408 [25] D.B. Snow. The Recrystallization of Heavily-Drawn Doped Tungsten Wire. *Metallurgical Transactions*
409 *A*. 7A:783-794 , 1976.
- 410 [26] M. Hillert. On the theory of normal and abnormal grain growth. *Acta Metallurgica*, 13:227-238, 1965.
- 411 [27] J.A. Mullendore. The technology of doped-tungsten wire manufacturing. In The metallurgy of
412 doped/non-sag tungsten. *Elsevier Applied Science*, 1989
- 413 [28] E. Pink, and I. Gaal. Mechanical properties and deformation mechanism of non-sag tungsten wires. In
414 The metallurgy of doped/non-sag tungsten. *Elsevier Applied Science*, 1989